Analyst

Accepted Manuscript

ROYAL SOCIETY OF CHEMISTRY

www.rsc.org/analyst

Journal Name

RSCPublishing

ARTICLE

Terbium (III)/gold nanoclusters conjugates: the development of a novel ratiometric fluorescent probe for mercury (II) and a paper-based visual sensor

Cite this: DOI: 10.1039/x0xx00000x

Received 00th January 2012,
Accepted 00th January 2012

DOI: 10.1039/x0xx00000x

www.rsc.org/

Yan-Xia Qi, Min Zhang*, Anwei Zhu, Guoyue Shi

In this work, a novel ratiometric fluorescent probe was developed for rapid, highly accurate, sensitive and selective detection of mercury (II) (Hg^{2+}) based on terbium (III)/gold nanoclusters conjugates (Tb^{3+}/BSA-AuNCs), in which bovine serum albumin capped gold nanoclusters (BSA-AuNCs) acted as the signal indicator and terbium (III) (Tb^{3+}) used as the build-in reference. Our proposed ratiometric fluorescent probe exhibited unique specificity toward Hg^{2+} against other common environmentally and biologically important metal ions, and had high accuracy and sensitivity with a low detection limit to 1 nM. In addition, our proposed probe was effectively employed to detect Hg^{2+} in the biological samples from the artificial Hg^{2+}-infected rats. More significantly, an appealing paper-based visual sensor for Hg^{2+} was designed by the filter paper embedded with Tb^{3+}/BSA-AuNCs conjugates, and we have further demonstrated its feasibility for facile fluorescent sensing of Hg^{2+} in a visual format, in which only a handheld UV lamp is used. In the presence of Hg^{2+}, the paper-based visual sensor, illuminated by a handheld UV lamp, would undergo a distinct fluorescence color change from red to green, which can be readily observed with naked eyes even in trace Hg^{2+} concentrations. The Tb^{3+}/BSA-AuNCs-derived paper-based visual sensor is cost-effective, portable, disposable and easy-to-use. This work unveiled a facile approach for accurate, sensitive and selective measuring of Hg^{2+} with self-calibration.

1 Introduction

The detection of heavy metal ions has attracted more and more attention, since contamination of heavy metal ions may cause serious harm to human health and the environment.[1] Mercury is one of the most toxic metallic global pollutants and has received much attention. Mercury can accumulate in vital organs and tissues, such as the liver, brain and heart muscle, and it can damage the central nervous system, endocrine system[2,3] and other organs. Water soluble mercury is one of the most common forms, and it can be stably existed in water.[4] Therefore, it is essential to develop new techniques to monitor aqueous Hg^{2+} ions. In the past few years, various kinds of methods have been developed to detect Hg^{2+}, including inductively coupled plasma mass spectrometry (ICP-MS), atomic absorption spectrometry (AAS), liquid chromatography and so on,[5-8] but there are many limitations for these methods. They often need sophisticated equipment, complicated sample preparation processes and trained professionals, high costs and large amounts of samples, moreover, they are not well-suited for quick detection.

Among the approaches or techniques for Hg^{2+} sensing, the fluorescence detection is more attractive owing to its advantages like simplicity, high sensitivity, good selectivity and rapid response time. Plenty of fluorescent probes and sensors for detection of Hg^{2+} have been reported.[9-12] But most of the Hg^{2+} fluorescent probes work by monitoring of fluorescence at a single wavelength, based on the increase/decrease of the fluorescence intensity as the response signal. But one of the major problems with these probes is the accuracy of the fluorescence measurement when they are applied to practical applications in environmental and biological system, because the fluorescence intensity is easily affected by series of factors in the sample environment and instrumental fluctuations, resulting in the distortion of fluorescence signal data.[13] To solve these problems, few ratiometric fluorescent probes for Hg^{2+} have been developed,[14] in which the ratiometric measurement allows the simultaneous measurement of two fluorescence signals at different wavelengths, followed by the calculation of their intensity ratio to minimize the ambiguities on fluorescence signals, thus giving greater analytic accuracy relative to single-channel detection. In addition, although there is increasing concerns about the adverse biological effects of Hg^{2+}, few ratiometric fluorescent probes have been employed to monitor the Hg^{2+} in biological samples. Therefore, it is highly desirable to develop a facile, green (low-toxicity reagent use, low reagent consumption) and environmental-friendly probe with the

advantages of ratiometric fluorescence for the detection of Hg^{2+} in biological samples.

Gold nanoclusters (AuNCs), a new type of fluorescent nanomaterials, have been widely exploited in a wealth of fields, such as catalysis, sensors, and so on.[15] Many capping agents, such as proteins, are used to prepare highly fluorescent AuNCs.[16] Bovine serum albumin (BSA) is the protein that most commonly used for the preparation of AuNCs. There are many approaches for synthesizing AuNCs utilizing BSA.[17] Xie *et al* synthesized BSA capped red-emitting AuNCs (BSA-AuNCs) using conventional heating method.[17a] Baker *et al* prepared oxidized BSA capped AuNCs (oxBSA-AuNCs) with two emission peaks by microwave (MW) irradiation, and furthermore they developed a "red"-emission-quenching assay for Hg^{2+} using oxBSA-AuNCs formed by microwave (MW) irradiation, in which the "blue" fluorescence signal arising from oxidized BSA was exploiting as an internal reference for a ratiometric detection.[17b] Although the ratiometric detection of Hg^{2+} based on BSA-AuNCs has already been reported, it is also appealing to devise novel BSA-AuNCs-based ratiometric fluorescent probes for Hg^{2+} by employing other strategies. As mentioned above, the BSA-AuNCs prepared by conventional heating method can be illuminated to fluoresce with only red emission. In addition, it is reported that BSA can sensitize trivalent terbium ion (Tb^{3+}) to fluoresce with green emission.[18] Enlightened by the facts, in this work, the integration of Tb^{3+} and BSA-AuNCs can form a novel fluorescent material (i.e., Tb^{3+}/BSA-AuNCs conjugates), which exhibited two major emission peaks (i.e., "green" and "red") at 548 nm and around 666 nm with excitation at 290 nm. However, in the presence of Hg^{2+}, the fluorescence of the Tb^{3+}/BSA-AuNCs conjugates was found to be quenched at around 666 nm ("red" emission) by Hg^{2+} and constant at 548 nm ("green" emission) (Scheme 1). Thus, a novel ratiometric fluorescent probe can be developed for the detection of Hg^{2+} based on Tb^{3+}/BSA-AuNCs conjugates, in which BSA-AuNCs acted as the signal indicator and Tb^{3+} used as the build-in reference.

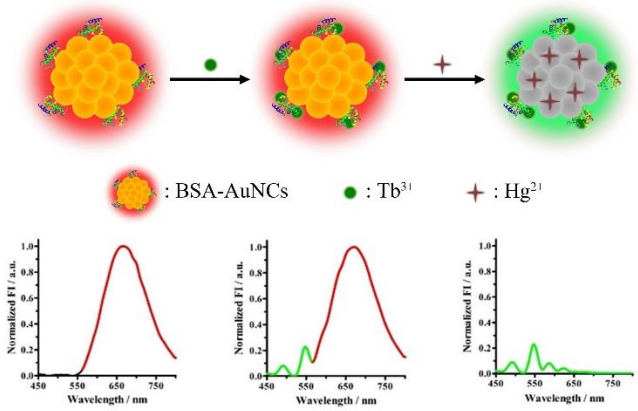

Scheme 1. Schematic illustration of our proposed ratiometric fluorescent probe based on the Tb^{3+}/BSA-AuNCs conjugates.

2 Experimental

2.1 Reagents and Materials. Hydrogen tetrachloroaurate (III) dehydrate ($HAuCl_4$) was purchased from Sinopharm Chemical Reagent Company (Shanghai, China). Terbium (III) nitrate hexahydrate was purchased from Diyang Chemical (Shanghai) Co. Ltd. Bovine serum albumin (BSA) was purchased from Sigma-Aldrich (St. Louis, MO). Cellulose filter paper (qualitative, Φ7 cm) was purchased from Xinxing Special Paper Co. Ltd (Hangzhou, China). 10×Tris-HAc buffer (100 mM, pH 7.9) was prepared from metal-free reagents in distilled water purified by a Milli-Q water purification system. All chemicals used in this work were of analytical reagent and obtained from commercial sources and directly used without additional purification.

2.2 Instrumentation. Fluorescence spectra were measured in a fluorescence microplate reader (infinite M200 pro, TECAN, Switzerland). Photographs were taken with a digital camera. The excitation wavelength used was 290 nm for the emission spectra. X-ray photoelectron spectroscopy (XPS) spectra were obtained from a AXIS Ultra DLD spectrometer (Shimadzu-Kratos, Japan). Transmission electron microscopy (TEM) images were obtained using a JEOL2100F electron microscope (JEOL, Tokyo, Japan). The elemental analysis was performed with energy-dispersive X-ray spectrometer (EDX, X-Max Oxford, U.K.). Atomic absorption spectrometer AMA-254 (Advanced Mercury Analyzer, LECO Corporation, USA) was used to test the artificial infected rats samples. Ultraviolet visible (UV-vis) absorption spectrum was recorded by a CARY-50 Conc spectrometer (Varian, USA).

2.3 Preparation of red fluorescent BSA-AuNCs. All glasses were thoroughly washed with aqua regia (HCl : HNO_3 volume ration = 3 : 1) and rinsed thoroughly with Mill-Q water prior to use. BSA-AuNCs was prepared according to the reported method.[17a] Briefly, 5 mL of 10 mM $HAuCl_4$ aqueous solution was added to 5 mL of 50 mg/mL BSA aqueous solution under vigorous stirring. Two minutes later, 0.5 mL of 1 M NaOH aqueous solution was introduced, the mixed solution was incubated for 12 h at 37 °C. The color of the solution changed from light yellow to light brown, and then deep brown. After cooling to room temperature (RT), the solution was further dialyzed to remove the excess impurities in a 3.5 KD dialysis bag for 10 h to obtain the purified BSA-AuNCs solution. Then the solution was collected and stored at 4 °C for further use.

2.4 Preparation of Tb^{3+}/BSA-AuNCs probe. It is reported that the carboxyl group of aspartic acid and glutamic acid on BSA can combine with metal ions, and BSA can sensitize Tb^{3+} to fluoresce with green emission. Therefore, the Tb^{3+}/BSA-AuNCs probe can be prepared based on the interaction of BSA-AuNCs and Tb^{3+}. More specifically, the Tb^{3+}/BSA-AuNCs probe was prepared by mixing 100 μL the purified BSA-AuNCs and 400 μL Tb^{3+} (1 mM). After incubated for 30 min, the mixture was further purified and collected by a 3 kDa MWCO centrifuge filter (Millipore) with several runs of the dilution and concentration cycles (centrifuged at 3000 rpm for 30 min in a run). The resultant Tb^{3+}/BSA-AuNCs were produced with fluorescence emission at 548 nm and around 666 nm with excitation at 290 nm. This as-prepared Tb^{3+}/BSA-AuNCs were stored at 4 °C for further use.

2.5 Assays for Hg^{2+} in biological samples. All procedures involving animals were conducted with the approval of the Animal Ethics Committee in East China Normal University, China. The kidney/liver were taken from the artificial infected rats, and the detailed process for the preparation of the artificial infected rats could be found in the supporting information. The kidney/liver were digested with a high-pressure method according to the reported literature.[19] Briefly, a certain amount of kidney/liver, concentrated HNO_3 (7 mL) and 30% H_2O_2 (2 mL) were sealed into a Teflon equipped stainless steel autoclave, which was then placed in a drying oven, followed by

hydrothermal treatment at 130 °C for 4 h. The autoclave was then cooled to RT. The obtained solution was subjected to evaporate its containing acid on an electric heating plate. A 100 μL mixture containing 50 μL the as-prepared Tb^{3+}/BSA-AuNCs, 10 μL Tris-HAc buffer (100 mM Tris, pH=7.9) and 40 μL the biological sample solution was prepared and incubated for 5 min at RT. Then, 90 μL of the mixture was used to be measured under the excitation wavelength at 290 nm.

2.6 Preparation of the paper-based visual sensor. A piece of cellulose filter paper was placed in a tweezer. 0.1 mL of the stock solution of Tb^{3+}/BSA-AuNCs conjugates was dripped into the filter paper. Then, the filter paper was naturally dried to form the paper-based visual sensor for Hg^{2+}. After that, 50 μL of Hg^{2+} solution with different concentrations was dripped into the as-prepared visual sensors, the visual sensors were placed at RT to evaporate the solvent thoroughly for further assay.

3 Results and discussion

3.1 Characterization of BSA-AuNCs and Tb^{3+}/BSA-AuNCs. The absorption and fluorescence emission were investigated to confirm the formation of AuNCs (Figure S1A). The maximum excitation and emission peak was observed at 386 nm and 666 nm, respectively. We also conducted the oxidation state of the as prepared BSA-AuNCs by X-ray photoelectron spectroscopy (XPS). As shown in Figure S1B, the binding energies of Au $4f_{7/2}$ could be deconvoluted into two parts centered at 83.88 eV and 85.0 eV, which could be assigned to Au^0 and Au^+, respectively. The result suggested that both of Au^0 and Au^+ existed in the BSA-stabilized clusters.[20] The as-prepared BSA-AuNCs were highly dispersed in aqueous solution, and a typical transmission electron microscopy (TEM) image in Figure S1C showed that they were monodispersed and uniform. The energy-dispersive X-ray (EDX) analysis showed that the chemical composition of BSA-AuNCs, and there was the characteristic peak of Au shown in the spectra of BSA-AuNCs (Figure S1D).

The Tb^{3+}/BSA-AuNCs conjugates were prepared based on the interaction of Tb^{3+} and BSA-AuNCs (see Experimental Section). The as-prepared Tb^{3+}/BSA-AuNCs exhibited three emission peaks at 494 nm, 548 nm and around 666 nm with excitation at 290 nm (Figure S2A). The two emission peaks at 494 nm and 548 nm were typically the characteristic peaks of Tb^{3+}. The chemical compositions of Tb^{3+}/BSA-AuNCs were also analyzed by the EDX spectrograph. The characteristic peaks of Au and Tb were shown in the spectra of the as-prepared Tb^{3+}/BSA-AuNCs (Figure S2B). The results indicated that Tb^{3+} was involved in the formation of Tb^{3+}/BSA-AuNCs conjugates by the interplay of Tb^{3+} and BSA.[18] A typical TEM image in Figure S2C showed that the size of the Tb^{3+}/BSA-AuNCs conjugates became a little larger than the pure BSA-AuNCs, which was also evidenced with the results from dynamic light scattering (DLS) (Figure S1E and Figure S2D). This might be due to the strong interaction of Tb^{3+} and BSA-AuNCs, resulting in self-aggregation to certain extend.

3.2 Ratiometric fluorescence assay for Hg^{2+} using the Tb^{3+}/BSA-AuNCs probe. Previous studies have reported that there were highly specific and strong dispersion forces between the closed-shell metal atoms, and relativistic effects played important role in magnifying the forces,[8,21] especially when these interactions involved heavy metal ions such as Au^+ and Hg^{2+}. From the data of the X-ray photoelectron spectroscopy (XPS) (Figure S1B), we knew that the amount of Au^+ on the surface of the BSA-AuNCs was about 21%, and this might be greatly magnify the matallophilic interactions between the Hg^{2+} and the Au^+, thus the interactions would cause the quenching the fluorescence of BSA-AuNCs.[22]

In the presence of Hg^{2+}, the fluorescence of the Tb^{3+}/BSA-AuNCs probe was found to be quenched at around 666 nm (i.e., the fluorescence of BSA-AuNCs), while the emission at 548 nm (i.e., the fluorescence of Tb^{3+} sensitized by BSA) remained constant. All the four characteristic peaks of Tb^{3+} at 494 nm, 548 nm, 585 nm, and 620 nm were displayed when the Tb^{3+}/BSA-AuNCs probe quenched at around 666 nm by Hg^{2+}. The resultant ratios of the fluorescence at 548 nm and 666 nm (F_{548}/F_{666}) should be related to the concentration of Hg^{2+}. The resultant ratiometric fluorescent response could provide a novel sensory probe for the determination of Hg^{2+}.

Considering the ratiometric changes in fluorescent properties of Tb^{3+}/BSA-AuNCs toward Hg^{2+}, the sensitivity of the proposed ratiometric fluorescent probe for analytical determination of Hg^{2+} was assessed. The Tb^{3+}/BSA-AuNCs probe was challenged with the different concentrations of Hg^{2+} from one stock solution. As shown in Figure 1A, with the addition of an increasing concentration of Hg^{2+} to Tb^{3+}/BSA-AuNCs probe solution, the fluorescence of Tb^{3+}/BSA-AuNCs probe at 666 nm was gradually quenched while the fluorescence at 548 nm remained constant. As presented in Figure 1B, the fluorescence intensity ratio (F_{548}/F_{666}) was sensitive to the concentration of Hg^{2+}, and it increased with the concentration of Hg^{2+} from 0.005 to 7 μM with a Boltzmann sigmoidal equation Y= –0.6490 + 13.2590 / [1 + exp (2.944 – X) / 1.058], where Y was the fluorescence ratio (F_{548}/F_{666}) and X was the concentration of Hg^{2+} (regression coefficient R^2=0.9956). The detection limit of Hg^{2+} using Tb^{3+}/BSA-AuNCs probe was 1 nM, which was lower than the maximum contaminant level of mercury in drinking water established by the World Health Organization.[23] The kinetics ratiometric fluorescence change of the Tb^{3+}/BSA-AuNCs probe toward Hg^{2+} was monitored, and it could be finished within 5 min (Figure S3). From the above, the Tb^{3+}/BSA-AuNCs probe demonstrates superior sensitivity and rapid response.

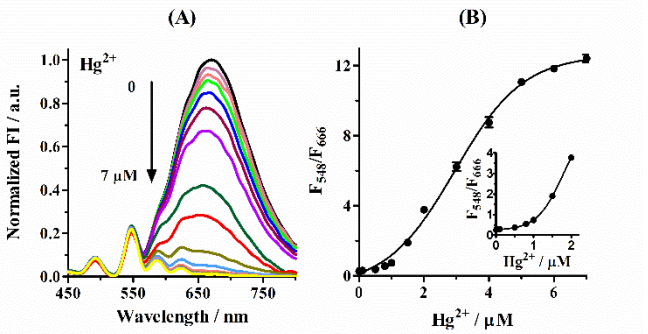

Figure 1. (A) Fluorescence responses of the Tb^{3+}/BSA-AuNCs probe to Hg^{2+}. The fluorescence emission spectra are shown for various Hg^{2+} concentrations (0, 0.005, 0.01, 0.05, 0.1, 0.5, 0.8, 1, 1.5, 2, 3, 4, 5, 6, and 7 μM). (B) Plot of fluorescence ratios (F_{548}/F_{666}) of the Tb^{3+}/BSA-AuNCs probe to the various concentrations of Hg^{2+} indicated.

Selectivity is a very important parameter to assess the performance of a fluorescent probe. To evaluate the selectivity of our proposed Tb^{3+}/BSA-AuNCs probe, we examined the fluorescence intensity ratio (F_{548}/F_{666}) in the presence of 10 μM other common environmentally and biologically important metal ions under the same conditions, including Ag^+, Ca^{2+}, Co^{2+},

Cu^{2+}, Cd^{2+}, K^{+}, Na^{+}, Ni^{2+}, Fe^{2+}, Hg^{2+}, Mn^{2+}, Mg^{2+}, Fe^{3+}, and Al^{3+}. Compared to the response of 5 μM Hg^{2+}, no obvious signals from other metal ions were observed, which showed the good selectivity of our proposed probe for Hg^{2+} over other metal ions (Figure 2A).

In addition, the advantages of the ratiometric fluorescent probe for Hg^{2+} can be validated in comparison to a single fluorescence quenching experiment, in which only a BSA-AuNCs probe was utilized for the measurement of Hg^{2+}. Compared with only BSA-AuNCs probe, our proposed ratiometric probe possess excellent performance to selective assay for Hg^{2+} (Figure S4), while the introduction of Tb^{3+} to the BSA-AuNCs probe could significantly improve its selectivity ability toward Hg^{2+} by the ratiometric format (Figure 2A). In order to further demonstrate the excellent selectivity of our proposed probe, competition experiments were conducted in the presence of Hg^{2+} mixed with other metal ions. Figure 2B revealed that the F_{548}/F_{666} of our probe in the presence of 5 μM Hg^{2+} mixed with 10 μM other metal ions was similar to that of in the presence of 5 μM Hg^{2+} alone. The results suggested that the coexistence of other metal ions had no effect on the detection of Hg^{2+} using our proposed probe, which demonstrated that our proposed ratiometric fluorescent probe can provide greater analytic accuracy relative to single-channel detection. The analytical performance of the present Hg^{2+} sensing system was compared with some of the reported methods for Hg^{2+} detection (Table S1). The Tb^{3+}/BSA-AuNCs system is more sensitive than the reported approaches.

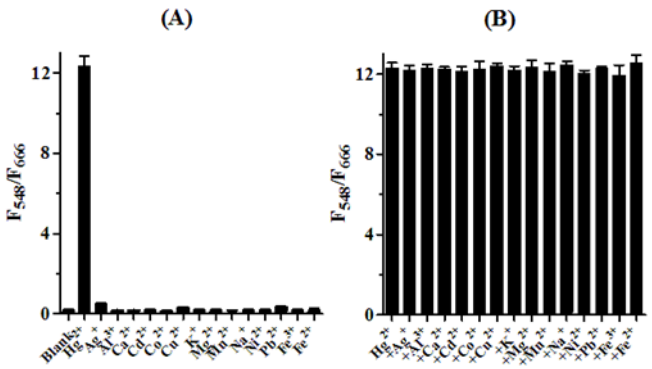

Figure 2. (A) Fluorescence ratios (F_{548}/F_{666}) of the Tb^{3+}/BSA-AuNCs probe to Hg^{2+} (5 μM) and various metal ions (10 μM). (B) Bars represent the F_{548}/F_{666} of the Tb^{3+}/BSA-AuNCs probe in the presence of 5 μM Hg^{2+} mixed with 10 μM other metal ions.

3.3 Visual assays for Hg^{2+} using our designed paper-based sensor. Contamination of the environment with Hg^{2+} has become a global concern for many years. The annual total global mercury emission from all natural and human-generated estimated by the U.S. Environmental Protection Agency (EPA) sources is ca. 7500 tons per year.[24] To some extent, the traditional methods for sensing Hg^{2+} are usually restricted by the requirement of expensive instruments or sophisticated operations. Thus, the development of a simple and quick method for the detection of Hg^{2+} is very important.

Herein, a novel paper-based visual sensor, consisted of the filter paper embedded with Tb^{3+}/BSA-AuNCs, for convenient monitoring of Hg^{2+} was developed, which can be applied to visually sensing Hg^{2+} under an UV lamp excitation (Figure 3A). In the presence of Hg^{2+}, the paper-based visual sensor, illuminated by a handheld UV lamp, would undergo a distinct fluorescence color change from red to green, which can be readily observed with naked eyes. Since the limit of detection (LOD) can be defined as the least amount of Hg^{2+} able to produce a different fluorescence color change that can be confirmed by the independent observers, the current LOD for Hg^{2+} thus is found to be as low as 0.1 μM with naked eyes using our proposed paper-based visual sensor (Figure 3B). Earlier work reported by Baker *et al*[17b] also used paper-based indicator strips immobilized with oxBSA-AuNCs for Hg^{2+} sensing, in which Hg^{2+} gave the most pronounced visual quenching at the lowest concentration of 0.1 mM. While using our proposed paper-based visual sensor, the detection of lowest concentration for Hg^{2+} could be as low as 0.1 μM observed by the naked eyes, which is about 3 orders of magnitude higher than that of the earlier work. In this respect, our proposed paper-based visual sensor may by more dominant in practical application. The Tb^{3+}/BSA-AuNCs-derived paper-based visual sensor is cost-effective, portable, disposable and easy-to-use, which has great potential for practical application and would satisfy the great demand for Hg^{2+} determination in fields such as water equality monitoring, pharmaceuticals, clinical analysis and food processing.

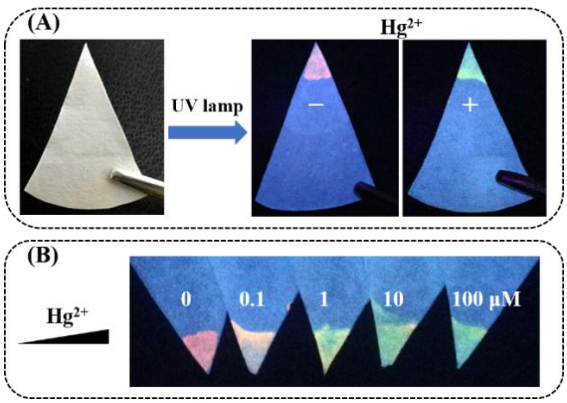

Figure 3. (A) Facile operational method for visual assay of Hg^{2+} based on the Tb^{3+}/BSA-AuNCs-derived paper-based visual sensor. (B) Fluorescence color image of the designed Hg^{2+}-indicating visual sensor after dropping 50 μL Hg^{2+} solution at different concentrations (0, 0.1, 1, 10, and 100 μM) under 254 nm UV light excitation.

3.4 Assays for Hg^{2+} in biological samples. We further applied the afore-mentioned method to detect Hg^{2+} in rat samples for evaluating the applicability of our proposed probe. The artificial Hg^{2+}-infected rats were prepared, and the Hg^{2+} content in the digested viscera samples from these rats was measured by using our proposed probe. The traditional atomic absorption (AAS) spectrometer AMA-254 (i.e., Advanced Mercury Analyser) was used as a standard method to evaluate the accuracy of our ratiometric fluorescent probe. As summarized in Table S2, the concentrations of Hg^{2+} in rat digested viscera samples determined by our method were compared with those obtained by AAS method. According to the statistic calculation by a *t* test (a = 0.1) (calculation of *t* value was shown in supporting information), the concentrations of Hg^{2+} determined by the present method were in good agreement with those obtained by the AAS method (t = 0.03 for kidney at low dose, t = 0.19 for liver at low dose, t = 0.02 for kidney at high dose, t = 0.03 for liver at high dose, which are smaller than standard t value of 2.13). These results can

effectively prove that the probe is likely to be capable of detecting Hg^{2+} in complex biological samples.

4 Conclusions

In summary, a ratiometric fluorescence probe for Hg^{2+} was developed based on Tb^{3+}/BSA-AuNCs conjugates, in which BSA-AuNCs acted as the signal indicator and Tb^{3+} used as the build-in reference. The ratiometric fluorescence probe provided high selectivity for Hg^{2+} over other common environmentally and biologically important metal ions, and possessed good sensitivity. This novel Tb^{3+}/BSA-AuNCs probe offered many advantages, including simplicity of preparation and manipulation, compared to other methods that employ specific strategies for Hg^{2+} detection. Moreover, the build-in correction by the ratiometric fluorescence probe can be provided to reduce background interference from environmental effects, thus greater analytic accuracy can be realized. We also applied this method to the detection of Hg^{2+} in the digested viscera samples from the artificial Hg^{2+}-infected rats and achieved convinced results successfully, which showed its great potential for practical application. Significantly, a novel paper-based visual sensor for Hg^{2+} was designed by the filter paper embedded with Tb^{3+}/BSA-AuNCs conjugates, and we can distinguish the Hg^{2+} content from the changed fluorescence color of the designed visual sensor directly with naked eyes under a hand-held UV lamp, which is convenient for point-of-care and in-field detection in view of avoiding the need of expensive instruments or professional operations. Our work established a reliable and accurate approach to determination of Hg^{2+}, and opened new avenues for the design of more novel sensing strategies and expansion of its application in various fields.

Acknowledgements

This work is supported by the National Natural Science Foundation of China (21275055, 21405047, and 21405048), China Postdoctoral Science Foundation (2014M550224, and 2014M550225) and large instruments Open Foundation of East China Normal University.

Notes and references

Department of Chemistry, School of Chemistry and Molecular Engineering, East China Normal University, 500 Dongchuan Road, Shanghai 200241, China. Email: mzhang@chem.ecnu.edu.cn; Tel&Fax: +86-21-54340042.

Electronic Supplementary Information (ESI) available. See DOI: 10.1039/b000000x/

1 (a) P. J. J. Huang and J. Liu, *Anal. Chem.*, 2014, **86**, 5999-6005; (b) Y. X. Qi, M. Zhang, Q. Q. Fu, R. Liu and G. Y. Shi, *Chem. Commun.*, 2013, **49**, 10599-10601; (c) M. Zhang, Y. Q. Liu and B. C. Ye, *Analyst*, 2012, **137**, 601-607.

2 (a) Y. H. Lin and W. L. Tseng, *Anal. Chem.*, 2010, **82**, 9194-9200; (b) D. Wen, L. Deng, S. Guo and S. Dong, *Anal. Chem.*, 2011, **83**, 3968-3972; (c) B. C. Ye and B. C. Yin, *Angew. Chem., Int. Ed.*, 2008, **47**, 8386-8389; (d) D. Liu, W. Qu, W. Chen, W. Zhang, Z. Wang and X. Jiang, *Anal. Chem.*, 2010, **82**, 9606-9610.

3 (a) L. Deng, X. Y. Ouyang, J. Y. Jin, C. Ma, Y. Jiang, J. Zheng, J. S. Li, Y. H. Li, W. H. Tan and R. H. Yang, *Anal. Chem.*, 2013, **85**, 8594-8600; (b) H. Wei, Z. D. Wang, L. M. Yang, S. L. Tian, C. J. Hou and Y. Lu, *Analyst*, 2010, **135**, 1406-1410.

4 (a) T. Li, S. J. Dong and E. K. Wang, *Anal. Chem.*, 2009, **81**, 2144-2149; (b) Q. Wei, R. Nagi, K. Sadeghi, S. Feng, E. Yan, S. J. Ki, R. Caire, D. Tseng and A. Ozcan, *ACS Nano*, 2014, **8**, 1121-1129.

5 (a) W. Y. Wang, F. Yang and X. R. Yang, *ACS Appl. Mater. Interfaces*, 2010, **2**, 339-342; (b) X. P. Yan, X. B. Yin, D. Q. Jiang and X. W. He, *Anal. Chem.*, 2003, **75**, 1726-1732; (c) J. Nan and X. P. Yan, *Chem. Commun.*, 2010, **46**, 4396-4398.

6 G. K. Darbha, A. K. Singh, U. S. Rai, E. Yu, H. Yu and R. P. Chandra, *J. Am. Chem. Soc.*, 2008, **130**, 8038-8043.

7 C. Wang, C. S. Tao, W. Wei, C. Meng, F. Liu and M. J. Han, *Mater. Chem.*, 2012, **20**, 4635-4641.

8 Z. Q. Hu, C. S. Lin, X. M. Wang, L. Ding, C. L. Cui, S. F. Liu and H. Y. Lu, *Chem. Commun.*, 2010, **46**, 3765-3767.

9 (a) M. Zhang, H. N. Le, X. Q. Jiang and B. C. Ye, *Chem. Commun.*, 2013, **49**, 2133-2135; (b) M. Zhang, B. C. Yin, W. Tan and B. C. Ye, *Biosens. Bioelectron.*, 2011, **26**, 3260-3265.

10 (a) Y. H. Lin and W. L. Tseng, *Anal. Chem.*, 2010, **82**, 9194-9200; (b) C. C. Huang, Z. Yang, K. H. Lee and H. T. Chang, *Angew. Chem., Int. Ed.*, 2007, **119**, 6948-6952.

11 (a) C. B. Huang, H. R. Li, Y. Y. Luo and L. Xu, *Dalton Trans.*, 2014, **43**, 8102; (b) H. L. Un, C. B. Huang, C. Huang, T. Jia, X. L. Zhao, C. H. Wang, L. Xu and H. B. Yang, *Org. Chem. Front.*, 2014, **1**, 1083.

12 J. Xie, Y. Zheng and J. Y. Ying, *Chem. Commun.*, 2010, **46**, 961-963.

13 (a) M. Zhang, H. N. Le, X. Q. Jiang, S. M. Guo, H. J. Yu and B. C. Ye, *Talanta*, 2013, **117**, 399-404; (b) C. Yu, M. Luo, F. Zeng, F. Zheng and S. Wu, *Chem. Commun.*, 2011, **47**, 9086-9088.

14 (a) M. Kumar, N. Kumar and V. Bhalla, *Dalton Trans.*, 2011, **40**, 5170-5175;(b) X. Wan, T. Liu and S. Liu, *Langmuir*, 2011, **27**, 4082-4090; (c) S. Yang, W. Yang, Q. Guo, T. Zhang, K. Wu and Y. Hua, *Tetrahedron*, 2014, **70**, 8914-8918.

15 (a) M. Zhuang, C. Ding, A. Zhu and Y. Tian, *Anal. Chem.*, 2014, **86**, 1829-1836; (b) Y. Wang, J. T. Chen and X. P. Yan, *Anal. Chem.*, 2013, **85**, 2529-2535; (c) J. Peng, L. N. Feng, K. Zhang, X. H. Li, L. P. Jiang and J. J. Zhu, *Chem. Eur. J.*, 2012, **18**, 5261-5268; (d) J. Sun, F. Yang, D. Zhao and X. R. Yang, *Anal. Chem.*, 2014, **86**, 7883-7889; (e) H. Kawasaki, K. Yoshimura, K. Hamaquchi and R. Arakawa, *Anal. Sci.*, 2011, **27**, 591-596.

16 (a) F. Wen, Y. Dong, L. Feng, S. Wang, S. Zhang and X. Zhang, *Anal. Chem.*, 2011, **83**, 1193-1196; (b) D. Lee, R. L. Donkers, G. Wang, A. S. Harper and R. W. Murray, *J. Am. Chem. Soc.*, 2004, **126**, 6193-6199.

17 (a) J. Xie, Y. Zheng and J. Y. Ying, *J. Am. Chem. Soc.*, 2009, **131**, 888-889; (b) C. M. Hofmann, J. B. Essner, G. A. Baker and S. N. Baker, *Nanoscale*, 2014, **6**, 5425-5431.

18 Y. Jin, W. Li and Q. Wang, *Biochem. Biophys. Res. Commun.*, 1991, **177**, 474-479.

19 M. Wang, J. Long, B. Yang, Y. Xu, H. Chen and Z. Zhou, *Environmental Chem.*, 2013, **32**, 893-897.

20 X. L. Guevel, B. Hotzer, G. Jung and M. Schneider, *J. Mater. Chem.*, 2011, **21**, 2974-2981.

21 A. Burini, J. P. Fackler, Jr. R. Galassi, T. A. Grant, M. A. Omary, M. A. Rawashdeh-Omary, B. R. Pietroni and R. J. Staples, *J. Am. Chem. Soc.*, 2000, **122**, 11264-11265.

22 (a) D. Hu, Z. Sheng, P. Gong, P. Zhang and L. Cai, *Analyst*, 2010, **135**, 1411-1416; (b) P. Yu, X. M. Wen, Y. R. Toh, J. Huang and J. Tang, *Part. Part. Syst. Charact*., 2013, **30**, 467-472.

23 Q. S. Wei, R. Nagi, K. Sadeghi, S. Feng, E. Yan, S. J. Ki, R. Caire, D. Tseng and A. Ozcan, *ACS Nano*, 2014, **8**, 1121-1129.

24 C. Y. Li, X. B. Zhang, L. Qiao, Y. Zhao, C. M. He, S. Y. Huan, L. M. Lu, L. X. Jian, G. L. Shen and R. Q. Yu, *Anal. Chem.*, 2009, **81**, 9993-10001.

